Chaos, Solitons and Fractals 142 (2021) 110513

Contents lists available at ScienceDirect

Chaos, Solitons and Fractals

Nonlinear Science, and Nonequilibrium and Complex Phenomena

journal homepage: www.elsevier.com/locate/chaos

Reconstruction of coupling structure in network of neuron-like oscillators based on a phase-locked loop

Marina V. Sysoeva [a,b], Ilya V. Sysoev [a,c,d,*], Mikhail D. Prokhorov [a], Vladimir I. Ponomarenko [a,d], Boris P. Bezruchko [a,d]

[a] Saratov Branch of Institute of Radioengineering and Electronics of Russian Academy of Sciences, 38, Zelyonaya str., Saratov, Russia
[b] Yuri Gagarin State Technical University of Saratov, 77, Politekhnicheskaya str., Saratov, Russia
[c] Lobachevsky State University of Nizhny Novgorod, 23, Gagarina av., Nizhny Novgorod, Russia
[d] Saratov State University, 83, Astrakhanskaya str., Saratov, Russia

ARTICLE INFO

Article history:
Received 30 August 2020
Revised 9 November 2020
Accepted 23 November 2020
Available online 29 November 2020

Keywords:
Network reconstruction
Time series
Neuro-oscillators
Phase-locked loop system

ABSTRACT

We study the problem of reconstructing the model equations for the network of 3rd order neuron-like oscillators from time series. The nodes of the network are phase-locked loop systems, which are able to exhibit different dynamical regimes including quasiharmonic oscillations, spiking, bursting, and chaotic behavior. Different network topologies are considered, including star, ring, chain, and random architectures.

A special approach using the idea of node nonlinear function continuity for constructing the target function is applied, which allows to reduce the model parametrization. Both the coupling parameters and parameters of individual nodes are estimated. Methods for the automatic noise reduction and superfluous coupling term removal are suggested and verified. These approaches provide a possibility to reconstruct the network topology even in the presence of a 10% measurement noise from the single scalar observable from each node in the case of different dynamical regimes and coupling architectures. This can find practical applications in neuroscience, in particular, for network reconstruction from experimental signals of individual cells.

1. Introduction

Reconstructing dynamical systems from time series (system identification) is a very well known inverse problem [1–4]. While a large number of different algorithms has been developed, we are still far beyond the general theory. After the first attempts to construct a general approach [5], it occurred that most successful techniques target some specific task, usually some particular class of systems like nonautonomous ordinary differential equations (ODEs, [6]), time-delay systems [7], stochastic phase oscillators [8,9], or oscillators which can have a limited (usually only two) number of states [10], including spiking systems for which only spiking and silence states are considered [11]. For all specific cases, using of a priori knowledge was always assumed [12]. There are also attempts to provide the theory for reconstruction of networks from event time series [13], when the complete continuous-time evolution is inaccessible. Some methods [14,15], being able to target many different types of systems, still need to know what type the considered object belongs to. The other methods need information about the structure of equations, but can either guess nonlinear function from a wide range of possible candidates [16–18] or reconstruct at least one nonlinear function as table-defined with no explicit equation for this function [19,20].

Here, we propose an approach to reconstruct a network of oscillators based on a phase-locked loop system [21], which were recently shown to exhibit neuron-like behavior [22,23]. Our interest to this system originates from the following practical reasons. First, this is the only known neuron-like 3rd order system in which all dynamical variables can be naturally obtained from the single observed variable by its numerical integration or differentiation, that is not possible for FitzHugh–Nagumo [24], Morris–Lecar [25], Hindmarsh–Rose [26] and other models [27]. Since real neurons often demonstrate complex behavior for individual nodes [28], networks of simple first-order relaxators reconstructed in Refs. [20,29] can be insufficient and 3rd order equations are much needed. Using hidden variable techniques developed for re-

* Corresponding author at: Saratov Branch of Institute of Radioengineering and Electronics of Russian Academy of Sciences, 38, Zelyonaya str., Saratov, Russia.
E-mail addresses: bobrichek@mail.ru (M.V. Sysoeva), ivssci@gmail.com (I.V. Sysoev), mdprokhorov@yandex.ru (M.D. Prokhorov), ponomarenkovi@gmail.com (V.I. Ponomarenko), bezruchkobp@gmail.com (B.P. Bezruchko).

https://doi.org/10.1016/j.chaos.2020.110513
0960-0779/

construction of single autonomous systems [30,31] for networks (including time delayed equations [32]) is not possible due to demands to solve the optimization problem in very large dimension.

Second, the neurooscillator proposed in the papers [22,23] has been already implemented in hardware [33]. If we aim to subsequently pass from reconstructing equations from their own numerical solution to the reconstruction of network from intra/extracellular recordings measured from real brain, it is better to have some intermediate stops to reveal and fix possible shortcomings step by step. A radio-engineering circuit may be the first step and a cell culture may be the second one.

Third, the system [22,23] was constructed in such a manner that the observed variable corresponding to a trans-membrane potential is a derivative of another variable and an antiderivative of the third one. It means that one of two unobserved variables can be obtained with a numerical differentiation and the other one with a numerical integration of the observable. Such an approach seems to be the optimal for a 3D system, while for 2D system considered in Ref. [19] there is no need in integration and for 1D systems, including time delayed systems considered in Ref. [34] there is no need in differentiation too. An approach, which requires to differentiate two times to obtain both unobserved variables, is more sensitive to noise. On the other hand, if it is neccessary to integrate two times to define the unobserved variables, it will force to take into account an unknown linear time trend in one of the variables. When only one antiderivative is used, we have to deal with a constant, but further we will show that an unknown constant is not a problem for our approach in contrast to a linear trend. Several approaches were specially designed for the reconstruction of stochastic equations [35], while the other used the Bayesian technique for the reconstruction of dynamic systems [36], but application of such methods to real neuroscience data is limited by relatively short time series length due to both insufficient time resolution in most neuroscience experiments and nonstationarity of biological systems.

To increase the robustness of the method, we will adapt the ideas of implicit (table) reconstruction of nonlinear function for each single oscillator, using the length of a line connecting the points of this function as a target function following [19,34], where the similar approaches were developed for the 2nd order differential equations and time-delay systems, respectively. Since we do not need any explicit approximation for a single node nonlinear function, such an approach gives us the following three significant advantages. First, the method robustness increases because it does not fail due to improper parametrization of the function, and fewer parameters have to be fitted for the model (mostly only parameters of coupling between the nodes have to be fitted). Second, the method becomes more general, since if the real nonlinear function is different from the model function proposed in the works [22,23] (we have to expect this situation), the method efficiency will not be affected. Third, the problem with an unknown constant in one of the variables rising from numerical integration of observable is solved (see below for details).

To distinguish between actual and superfluous connections in the network, we perform a step by step addition or elimination of coupling coefficients in the model using Fischer F-criterion. In contrary to Ref. [34], where such an approach was performed, elimination of spurious coupling terms was done for the whole ensemble (not individually for each reconstructed oscillator) and Bonferroni correction for significance was applied. In Ref. [19] no technique for reduction of superfluous connections was proposed.

Further we will show that the proposed technique is able to reconstruct the network of ten oscillators of type [22,23] for different architectures and to reveal both the network couplings and the nonlinear functions and parameters of individual nodes. Only scalar observable is necessary for each node, with a measurement noise being up to 10% by standard deviation. It is also shown how to overcome some problems specific for the considered neuron model.

2. Models and methods

2.1. Model and coupling architecture

We consider the model described by the following system of differential equations:

$$\begin{aligned} \frac{d\varphi}{dt} &= y, \\ \frac{dy}{dt} &= z, \\ \varepsilon_1\varepsilon_2\frac{dz}{dt} &= \gamma - (\varepsilon_1+\varepsilon_2)z - (1+\varepsilon_1\cos\varphi)y, \end{aligned} \tag{1}$$

where the variables φ and y are the instantaneous phase difference and the corresponding frequency difference between a tunable oscillator and a master oscillator, respectively, z is the velocity of changing of the phase difference y, the parameter γ defines an initial frequency detuning, and ε_1 and ε_2 are the parameters of control loop. In relation to neuron dynamics, the variable y can be interpreted as a variable describing a change in the membrane potential, the parameters ε_1 and ε_2 allow one to set the necessary dynamical regime, and γ has an effect similar to that of an external current in the Hodgkin–Huxley model [37].

Here, the phase-locked loop system was considered in four different regimes following [23]:

1. Quasiharmonic regime ($\gamma_i \in [0.26; 0.30]$, $\varepsilon_{i,1} \in [1; 3]$, and $\varepsilon_{i,2} = 10$);
2. Spiking regime ($\gamma_i \in [0.065; 0.085]$, $\varepsilon_{i,1} \in [4.5; 8]$, and $\varepsilon_{i,2} = 10$);
3. Bursting regime ($\gamma_i \in [0.185; 0.195]$, $\varepsilon_{i,1} \in [25; 29]$, and $\varepsilon_{i,2} = 10$);
4. Chaotic regime ($\gamma_i \in [0.24; 0.26]$, $\varepsilon_{i,1} \in [18; 21]$, and $\varepsilon_{i,2} = 10$).

In all four cases, we consider ensembles of ten coupled oscillators (2):

$$\begin{aligned} \frac{d\varphi_i}{dt} &= y_i, \\ \frac{dy_i}{dt} &= z_i, \\ \varepsilon_{i,1}\varepsilon_{i,2}\frac{dz_i}{dt} &= \gamma_i - (\varepsilon_{i,1}+\varepsilon_{i,2})z_i - (1+\varepsilon_{i,1}\cos\varphi_i)y_i + \sum_{j=1, j\neq i}^{D} k_{i,j}(y_j - y_i), \end{aligned} \tag{2}$$

where coefficients $k_{i,j}$ provide a matrix of couplings between individual oscillators (nodes), in which the number i is the number of a driven node (in a row) and the number j is the number of a driving node (in a column). The parameters $\varepsilon_{i,1}, \varepsilon_{i,2}$, and γ_i can be set different for different oscillators. The parameters γ_i and $\varepsilon_{i,1}$ were uniformly distributed in the corresponding range with smaller values corresponding to smaller oscillator number i.

Additive measurement normal noise was added to the system. The standard deviation of noise was 1%, 5%, and 10% of the standard deviation of the signal without noise that corresponded to the signal-to-noise ratio equal to 40 dB, 26 dB, and 20 dB, respectively.

Four types of coupling architectures were considered: chain, ring, star, and random couplings (Fig. 1). For three coupling architectures: chain, ring, and random couplings, all non-zero couplings were set the same and equal to $k = 0.01$. For a star, the coupling coefficients characterizing the coupling from the central oscillator to the peripheral oscillators were equal to $k = 0.02$, while the coupling coefficients characterizing the coupling in the opposite direction were equal to $k = 0.01$.

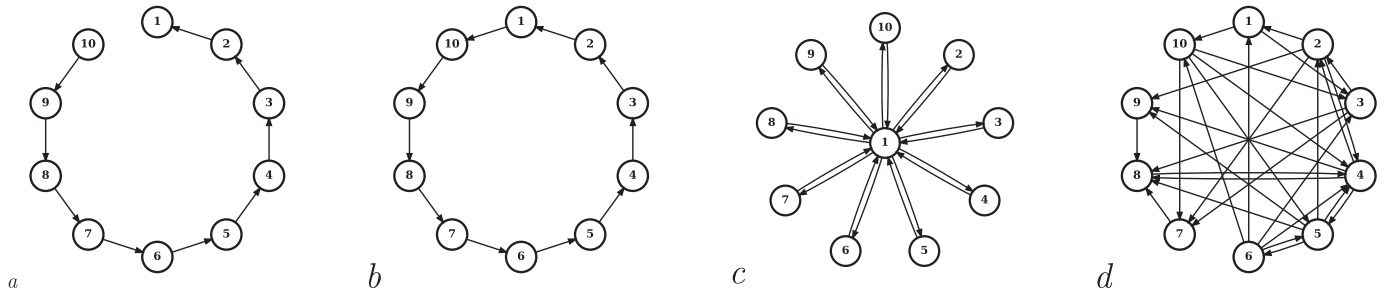

Fig. 1. Coupling architecture: *a*) Chain, *b*) Ring, *c*) Star, *d*) Random couplings.

It was shown in Ref. [19] that for oscillators in a periodic regime, the error in reconstructing their parameters from time series is greater than for oscillators in a chaotic regime. Moreover, in the case of the network reconstruction from periodic time series, several couplings can be missed [38]. The quality of coupling architecture reconstruction depends on the noise level and the oscillation regime [20]. We also assume that the method accuracy may depend on the coupling architecture in the network.

2.2. Reconstructing equations of single neuron

In the radioengineering experiment with phase-locked loop systems, the variable y is the only one measured [33]. The same variable corresponds to the membrane potential when Eq. (1) is considered as a neuron model. Therefore, the reconstruction task is formulated further in the way, that only the variable y is observed. To reconstruct the complete state vector, the variable z is obtained with numerical differentiation using smoothing polynomial, constructed from m data points. Usually, m is set depending on the measurement noise level under the assumption $3 \le m \le \frac{(T/\Delta t)}{8}$, where Δt is a sampling time, T is the minimal time scale over all time scales at which significant activity is demonstrated, measured in units of Δt. However, such an approach to m selection is not optimal, especially if different time scales are inherent to the signal. Therefore, we use another technique, which is described further. In the absence of noise and low noise levels, the minimal $m = 3$ value is suitable. The variable φ can be reconstructed by numerical integration using the Simpson method. Since this method requires parabolas to be constructed at time intervals of $2\Delta t$ (3 data points are necessary), let us assume N (the total number of data points in the measured time series) to be odd. If this is not the case, we remove the last data point.

Let us rewrite the last equation in Eq. (1) for the isolated oscillator (without coupling) in the following form:

$$\begin{aligned} &\tfrac{dz}{dt} = \alpha_0 + \alpha_1 z - f(\varphi) y, \\ &\alpha_0 = \tfrac{\gamma}{\varepsilon_1 \varepsilon_2}, \alpha_1 = -\tfrac{\varepsilon_1 + \varepsilon_2}{\varepsilon_1 \varepsilon_2}, \end{aligned} \tag{3}$$

where $f(\varphi)$ in general case is an unknown nonlinear continuous function. Thus, the unknown constant arising from the numerical integration used for obtaining the variable φ can be safely ignored. Also, let us consider the 2π-periodic phase φ in the range $0 \le \varphi < 2\pi$.

Following the ideas of Ref. [34], we construct a target function for the recovery of parameters α_0 and α_1, by minimizing the length of a line connecting the points of reconstructed nonlinear function f. This approach makes it unnecessary to expand the function f in a row. Therefore, the method becomes more general (it can be used for arbitrary f) and at the same time, the parametrization is sufficiently reduced (fewer number of coefficients α to be estimated), given better statistical properties of estimates for remaining coefficients. Let us rewrite Eq. (3), expressing f by other terms:

$$f(\varphi) = \alpha_0 \tfrac{1}{y} + \alpha_1 \tfrac{z}{y} - \tfrac{1}{y} \tfrac{dz}{dt}. \tag{4}$$

Time series of $\frac{dz}{dt}$ can be also calculated using numerical differentiation.

Then, we consider a sorting map $Q(n)$ (n is the number of data point in the time series), matching the number n in the original time series with the number $Q(n)$ in the time series sorted by increase of φ. An inverse map Q^{-1} matches the number of a point in the sorted time series with its number $Q^{-1}(Q(n)) = n$ in the original time series. Let us consider a data point located in the sorted time series immediately before the point with the number $Q(n)$. Such a point will have a number $Q^{-1}(Q(n) - 1)$ in the sorted time series, which we denote as p_n for convenience. Then, the increment of the function f on the interval $\big(\varphi(p_n); \varphi(n)\big)$ will be expressed as follows:

$$\begin{aligned} \delta_n = f(\varphi(n)) - f(\varphi(p_n)) &= -\Delta\zeta(n) + \alpha_0 \Delta y^{-1}(n) + \alpha_1 \Delta\upsilon(n), \\ \Delta\zeta(n) &= \frac{1}{y(n)} \frac{dz}{dt}(n) - \frac{1}{y(p_n)} \frac{dz}{dt}(p_n), \\ \Delta y^{-1}(n) &= \frac{1}{y(n)} - \frac{1}{y(p_n)}, \\ \Delta\upsilon(n) &= \frac{z(n)}{y(n)} - \frac{z(p_n)}{y(p_n)}. \end{aligned} \tag{5}$$

Note that n for which $Q(n) = 0$ (we numerate the points starting from zero, i. e. $n = 0, 1, \ldots, N-1$) is not allowed, since it does not have the corresponding p_n (there is no previous point in the time series because the value ϕ_n is minimal). After these preparations, the value L can be used as a target function:

$$L(\alpha_0, \alpha_1) = \sum_n \delta_n^2. \tag{6}$$

The quadratic dependence of L on α_0 and α_1 is obvious from (5). Thus, Eq. (5) can be considered as a formulation of a least square problem for approximation of $\Delta\zeta(n)$ with $\Delta y^{-1}(n)$ and $\Delta\upsilon(n)$, which can be considered as basis functions. In such a case, δ_n represents residuals. At the right choice of α_0 and α_1, the target function L is many times smaller than at the wrong choice of these parameters when f has discontinuities in almost all points.

Since even for the actual values of parameters α_0 and α_1 the target function stays nonzero $L > 0$ in general case, the estimates obtained with such a technique should be biased for any finite N. However, if the function f is continuous, then $\delta_n \to 0$ at $N \to \infty$, since $0 \le \varphi < 2\pi$, and the infinite number of measured values of $\varphi(n)$ will fill the finite range. If we additionally assume the function f to be differentiable in the range $0 \le \varphi < 2\pi$, then $\delta_n \to df(\varphi(p_n))$ and, therefore, δ_n is an approximation of f differential in the point $\varphi(p_n)$ from the right side or, alternatively, in the point $\varphi(n)$ from the left side, that gives the same for differentiable function in the limit. Then, $\lim\limits_{N\to\infty} L = \int (df)^2 =$

$\int \left(\frac{df}{d\varphi}\right)^2 (d\varphi)^2 = \left(\frac{df}{d\varphi}\right)^2 d\varphi \to 0$, providing asymptotically unbiased estimates of α_0 and α_1.

The proposed approach allows us to estimate α_0 and α_1, which are the combinations of the original parameters γ, ε_1, and ε_2. However, one can see from the third equation of the system (1) that separate estimation of γ, ε_1, and ε_2 becomes impossible when we switch to the function $f(\varphi) = 1 + \varepsilon_1 \cos\varphi$, since all terms have unknown coefficients including the term at the left-hand side of the equation. It means, that a possible system of equations constructed to estimate the coefficients will be ill-defined. Consequently, the proposed approach is not limited comparing with any other approach, which proposes an explicit expansion of the function $f(\varphi)$ in a row similar to Ref[5].

2.3. Reconstructing equations of coupled neurons

The proposed algorithm is promising for reconstructing a network (2) with a large number D of coupled oscillators (1), since it allows to reconstruct not only parameters of individual oscillator, but also coupling coefficients and reveal the coupling architecture.

To adapt the method to multiple nodes, we rewrite Eq. (4) as follows:

$$f_i(\varphi_i) = \alpha_{i,0}\frac{1}{y_i} + \alpha_{i,1}\frac{z_i}{y_i} - \frac{1}{y_i}\frac{dz_i}{dt} + \sum_{j=1,j\neq i}^{D} \beta_{i,j}\left(\frac{y_j}{y_i} - 1\right), \tag{7}$$

where $\alpha_{i,0}$ and $\alpha_{i,1}$ have the same sense as for individual node and additional coefficients $\beta_{i,j} = \frac{k_{i,j}}{\varepsilon_{i,1}\varepsilon_{i,2}}$ represent the coupling. The formula (5) is rewritten as follows:

$$\begin{aligned}
\delta_{i,n} &= f_i(\varphi_i(n)) - f_i(\varphi_i(p_{n,i})) = \\
&- \Delta\zeta_i(n) + \alpha_{i,0}\Delta y_i^{-1}(n) + \alpha_{i,1}\Delta\upsilon_i(n) + \sum_{j=1,j\neq i}^{D} \beta_{i,j}\Delta Y_{i,j}(n), \\
\Delta\zeta_i(n) &= \frac{1}{y(n)}\frac{dz}{dt}(n) - \frac{1}{y(p_{n,i})}\frac{dz}{dt}(p_{n,i}), \\
\Delta y_i^{-1}(n) &= \frac{1}{y_i(n)} - \frac{1}{y_y(p_{n,i})}, \\
\Delta\upsilon(n) &= \frac{z_i(n)}{y_i(n)} - \frac{z_i(p_{n,i})}{y_i(p_{n,i})}, \\
\Delta Y_{i,j}(n) &= \frac{y_j(n)}{y_i(n)} - \frac{y_j(p_{n,i})}{y_i(p_{n,i})}.
\end{aligned} \tag{8}$$

Here, the number $p_{n,i}$ has additional index i, since the sorting map $Q_i(n)$ is different for different nodes, meaning that the same n at different i is projected to different $p_{n,i}$. Using the new definition for $\delta_{i,n}$, the target function is written similar to the autonomous case (6) except the dependence on the coupling parameters:

$$L_i(\alpha_{i,0}, \alpha_{i,1}, \beta_{i,1}, \ldots, \beta_{i,D}) = \sum_n \delta_{i,n}^2. \tag{9}$$

Now, we have a specific target function L_i for each oscillator, which minimization leads to estimates for both parameters of intrinsic dynamics $\alpha_{i,0}$ and $\alpha_{i,1}$ and the coupling parameters $\beta_{i,j}$. Each oscillator is reconstructed independently from the others. The least squares originating from minimization of the target function (9) is linear and can be solved using a linear routine, it does not require use of simplex method as in Ref. [34]. Therefore, it does not require starting guesses to be set, demands much less time for calculation (usually 5–100 times less) and guarantees convergence to the global minimum.

2.4. Detection of insignificant couplings

For large enough D, the values $\delta_{i,n}$ are distributed by the law close to the normal one, since they are the sums of large number of similar elements. For $N \to \infty$, their mean tends to zero. Thus, their sum L_i should have the distribution close to χ^2 with $(N-1)$ degrees of freedom. However, it is not so due to the two reasons. First, the consequent $\delta_{i,n}$ are constructed partly from the same data and are not independent. It means that one half of values have to be ignored. Second, to calculate L_i, we used $(D+1)$ free parameters: two α_i and $(D-1)$ number of β_i. Using these properties, we construct the algorithm of sequential elimination of insignificant couplings from the model of ith oscillator.

First, we remove each coupling separately from the model (2) and construct $(D-1)$ reduced models. They will have a target function larger than the original full model. Among all the reduced models, we choose the one, for which the target function is minimal. For convenience, we denote as $\delta'_{i,n}$ the values similar to $\delta_{i,n}$, but calculated in the absence of one coupling term. Now, we can construct the value $\Lambda_{i,D-1}$ as a ratio of target function values for the full and reduced model:

$$\Lambda_{i,D-1} = \frac{\sum_{n=1}^{N/2} \delta_{i,2n}^2}{\sum_{n=1}^{N/2} \delta_{i,2n}'^2}, \tag{10}$$

where the lower index $(D-1)$ of $\Lambda_{i,D-1}$ means that it was obtained by elimination of one coupling from the full model (8). The value $\Lambda_{i,D-1}$ has to be distributed by the Fisher law. If the calculated value does not lie at the distribution tail, i. e. the inequality (11) is valid, it means that the target functions of full and reduced models are from the same distribution and the removed coupling term is superfluous and was removed rightly.

$$F_{\Lambda_{i,D-1}}\left(\frac{N}{2} - (D+1), \frac{N}{2} - D\right) < 1 - \frac{p}{D-1}, \tag{11}$$

where p is a confidence level, i.e. the probability to remove the coupling term erroneously, with the Bonferroni correction for $(D-1)$ couplings in the network.

If the reduced model is accepted, the procedure should be repeated testing the models with two removed couplings. Then, we remove three couplings and so on until the following inequality becomes valid:

$$F_{\Lambda_{i,r_i}}\left(\frac{N}{2} - (r_i+2), \frac{N}{2} - (r_i+1)\right) \geqslant 1 - \frac{p}{r_i}, \tag{12}$$

where r_i is the number of kept couplings for ith oscillator, with 2 and 1 placed in Eq. (12) after r_i due to parameters $\alpha_{i,0}$ and $\alpha_{i,1}$ responsible for the autonomous dynamics. Validity of Eq. (12) means that no more couplings should be removed.

The alternative approach is also possible. Let us start from the autonomous system and add coupling terms one by one. At each step, we construct all possible models with one extra coupling, but only one of them, which has the minimal target functions should be tested for significance. At the first algorithm step, when the first coupling is added to the autonomous system, we calculate the following ratio:

$$\Lambda_{i,1} = \frac{\sum_{n=1}^{N/2} \delta_{i,2n}^2}{\sum_{n=1}^{N/2} \delta_{i,2n}'^2}, \tag{13}$$

where δ_i^2 corresponds to the autonomous system and $\delta_i'^2$ corresponds to the system with one extra coupling. If the value $\Lambda_{i,1}$ belongs to the tail of the Fisher distribution, i. e. the inequality (14) takes place, then this coupling should be added to the model.

$$F_{\Lambda_{i,1}}\left(\frac{N}{2} - 3, \frac{N}{2} - 2\right) > 1 - p. \tag{14}$$

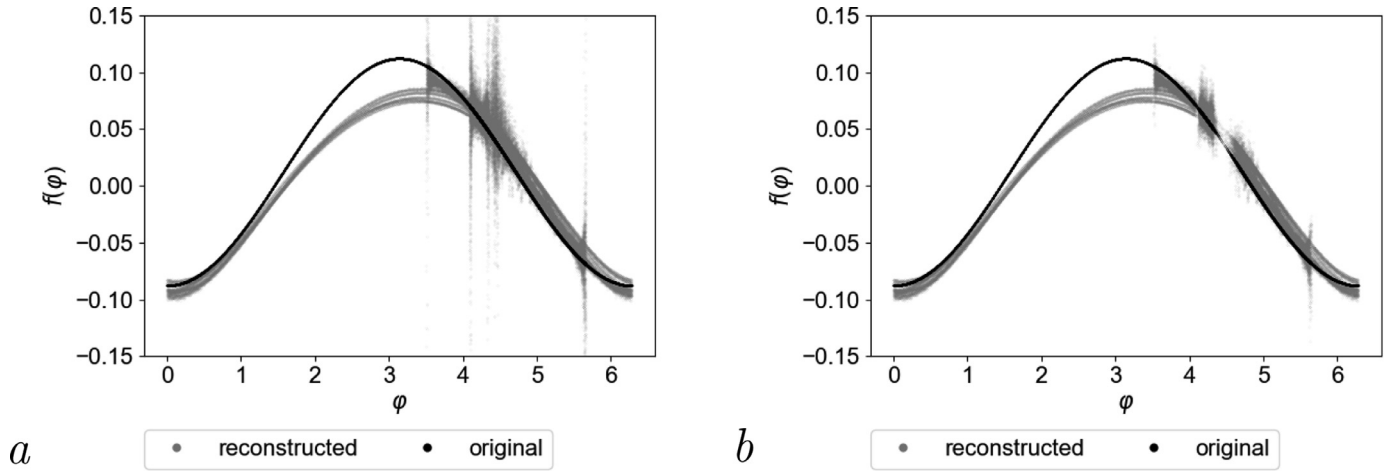

Fig. 2. Reconstructed nonlinear function of a neuron in bursting regime with added 1% noise. *a*) without removed points ($\nu = 0$); *b*) with removed points at $\nu = 0.2$.

Then, the second coupling term should be added into the model and tested in a similar way. This procedure is repeated until the adding of the term having the number $(r_i + 1)$ results in the following inequality:

$$F_{\Lambda_{i,r_i}}\left(\frac{N}{2} - (r_i + 3), \frac{N}{2} - (r_i + 2)\right) \leqslant 1 - p. \tag{15}$$

After that, no more couplings should be added and r_i couplings stay in the model.

3. Results

3.1. Reconstruction of state vector and model parameters for autonomous neuron

The Eq. (1) were solved by the 4th-order Adams' method with an adaptive integration step. The sampling interval was $\Delta t = 1/32$. A 1%, 5%, and 10% measurement noise was added to the time series. The absolute value of noise dispersion was different for different regimes and depended on the dispersion of the time series of y.

There is a division by zero in Eq. (5) for $y(n) = 0$ or for $y(p_n) = 0$. While precise zero is unlikely, all very small values of y are dangerous for the proposed technique, since the matrix of basis function values used at solving the least squares problem becomes ill-conditioned. Measurement noise can deteriorate this situation shifting some sampled values of y closer to zero. Therefore, there appears an additional method parameter, allowing to distinguish between appropriate $y(n)$ values and those, which are too close to zero. We can provide some absolute value ν, which should depend on the signal variance, with all δ_n for which $|y(n)| < \nu$ or $|y(p_n)| < \nu$ to be excluded from the target function (6). Some balance should be kept when choosing ν. Very small ν is obviously inappropriate since too many ill-defined rows stay in the basis function matrix. Very large ν leads to removal of most data from the least squares routine leading to two problems: first, statistical properties of estimates become worse, second, for many y, the nonlinear function will be not defined. The optimal value $\nu = 0.2$ was defined empirically, but it can be substantiated by the following ideas. If we remove about $1/3$ or $1/2$ of all $y(n)$, the statistical properties of parameter estimates should not deteriorate much, but all kept $y(n)$ will be of the same order. Fig. 2 shows how different ν values affect the results of nonlinear function reconstruction.

For reconstructing the model equations in the absence of noise, it is sufficient to use three points of time series for differentiation. When noise is added, the number of points required for smoothing at differentiation increases significantly. The optimal number of points m_{opt} used for differentiation was selected for each regime individually by minimizing the target function $L(m)$. The results of such calculations with added 1% noise are shown in Table 1. Such an approach does no demand any a priori knowledge and seems to be impartial because the decision is made based on unambiguous criterion, but needs a lot of calculations. It is interesting to note, that m_{opt} occurs to be significantly larger for periodic regime than for other considered regimes.

The reconstructed model parameters $\hat{\alpha_0}$ and $\hat{\alpha_1}$ at the optimal m_{opt} and relative errors of parameter estimation $\Delta\alpha_0$ and $\Delta\alpha_1$ are presented in Table 1. The relative errors were estimated as follows:

$$\Delta\alpha = \frac{|\alpha - \hat{\alpha}|}{\alpha}. \tag{16}$$

3.2. Reconstruction of coupling architecture

To objectively evaluate and compare the efficiency of the methods of elimination of couplings and addition of couplings, we analyze their sensitivity Eq. (17) and specificity Eq. (18):

$$sens = \frac{TP}{TP + FN} \cdot 100\%, \tag{17}$$

$$spec = \frac{TN}{TN + FP} \cdot 100\%. \tag{18}$$

The sensitivity is the proportion of actual positives, which are correctly identified. It is calculated out of the true positives (TP) and false negatives (FN) as described by Eq. (17). Specificity measures the proportion of negatives, which are correctly identified, and is calculated out of the true negatives (TN) and the false positives (FP) as defined by Eq. (18). For example, in Figs. 3 and 4, TP are shown as black squares, FN are shown as red squares, FP are shown as green squares, and TN are shown as white squares.

In the absence of measurement noise, the addition technique demonstrates poor specificity (68–98%) for all the considered regimes and architectures. While the sensitivity is 100% for the chain, ring, and random architectures, it is only 55% for the star architecture in the quasiharmonic regime. When the noise level is increased to 10%, the sensitivity remains at 100% for all regimes except quasiharmonic. Even for the relatively moderate 1% noise, two couplings are missed for the quasiharmonic regime, as it is shown in Fig. 3*a* in comparison to other regimes, see Fig. 3*b–d*. When different architectures are compared, the sensitivity is always lower for the star architecture, for which it drops to 0% for the quasiharmonic regime, when the 10% noise is added. For the moder-

Table 1
Reconstructed model parameters for single neuron with added 1% noise.

Regime	α_0	$\hat{\alpha_0}$	$\Delta\alpha_0$	α_1	$\hat{\alpha_1}$	$\Delta\alpha_1$	m_{opt}
Quasiharmonic	0.01	0.0092	8%	−0.4333	−0.0488	89%	463
Spiking	0.0011	0.0011	0%	−0.225	−0.2181	3%	167
Bursting	0.0007	0.0007	0%	−0.1345	−0.1274	5%	175
Chaotic	0.0012	0.0013	8%	−0.1476	−0.1399	5%	165

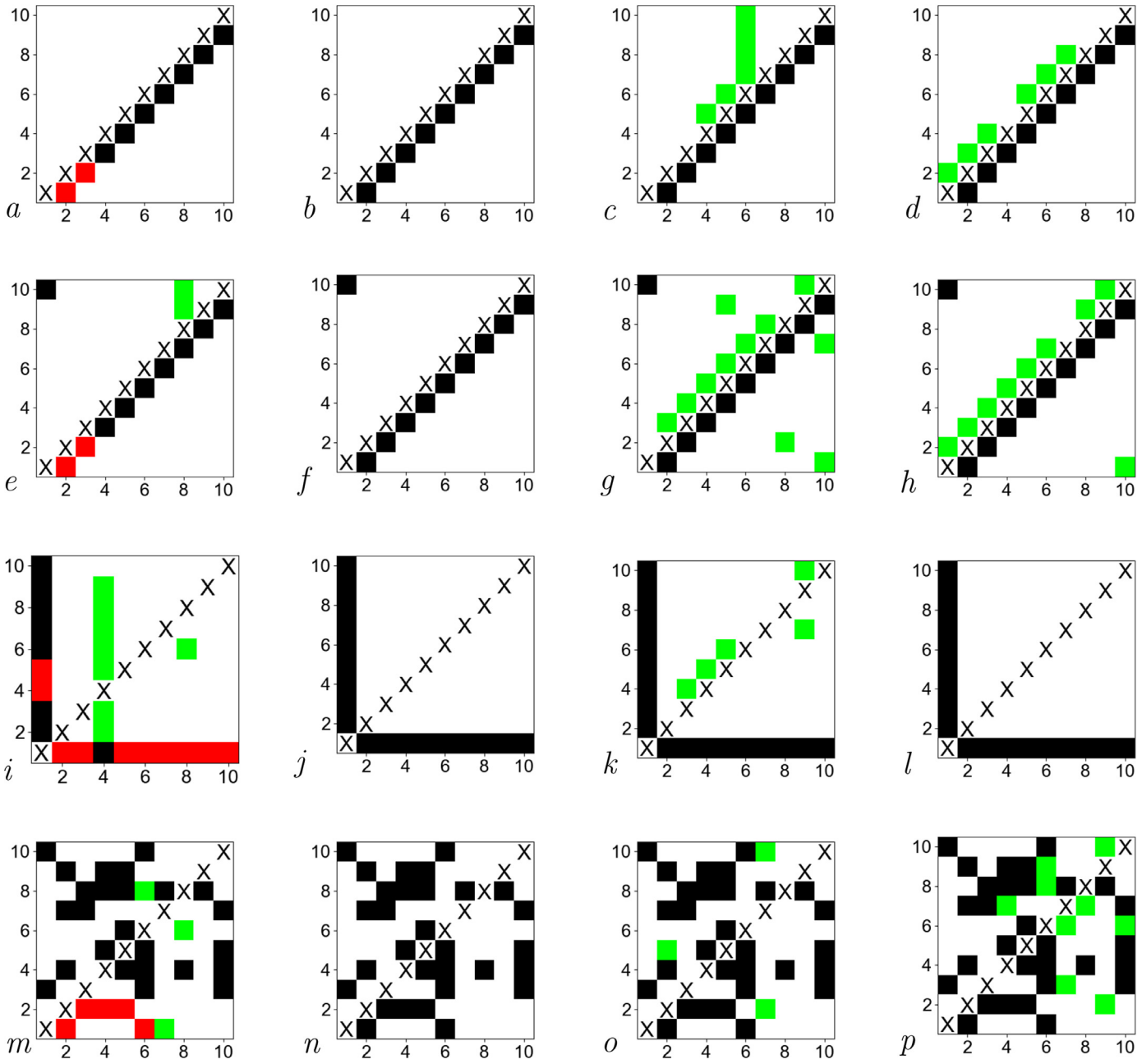

Fig. 3. Schemes of coupling architecture reconstruction using the method of addition of couplings in the presence of 1% measurement noise. The first, second, third, and fourth lines correspond to the chain (*a*–*d*), ring (*e*–*h*), star (*i*–*l*), and random architecture (*m*–*p*), respectively. The first, second, third, and fourth rows correspond to the quasiharmonic (*a*), (*e*), (*i*), and (*m*), spiking (*b*), (*f*), (*j*), and (*n*), bursting (*c*), (*g*), (*k*), and (*o*), and chaotic (*d*), (*h*), (*l*), and (*p*) regimes, respectively. The numbers of driving neurooscillators are shown on the horizontal axis, while the numbers of driven oscillators are shown on the vertical axis. The squares of different color correspond to detected existing couplings (black), removed from the model nonexisting couplings (white), absent by definition couplings to itself at $j = i$ (cross), spuriously detected couplings (green), and missed existing couplings (red). (For interpretation of the references to colour in this figure legend, the reader is referred to the web version of this article.)

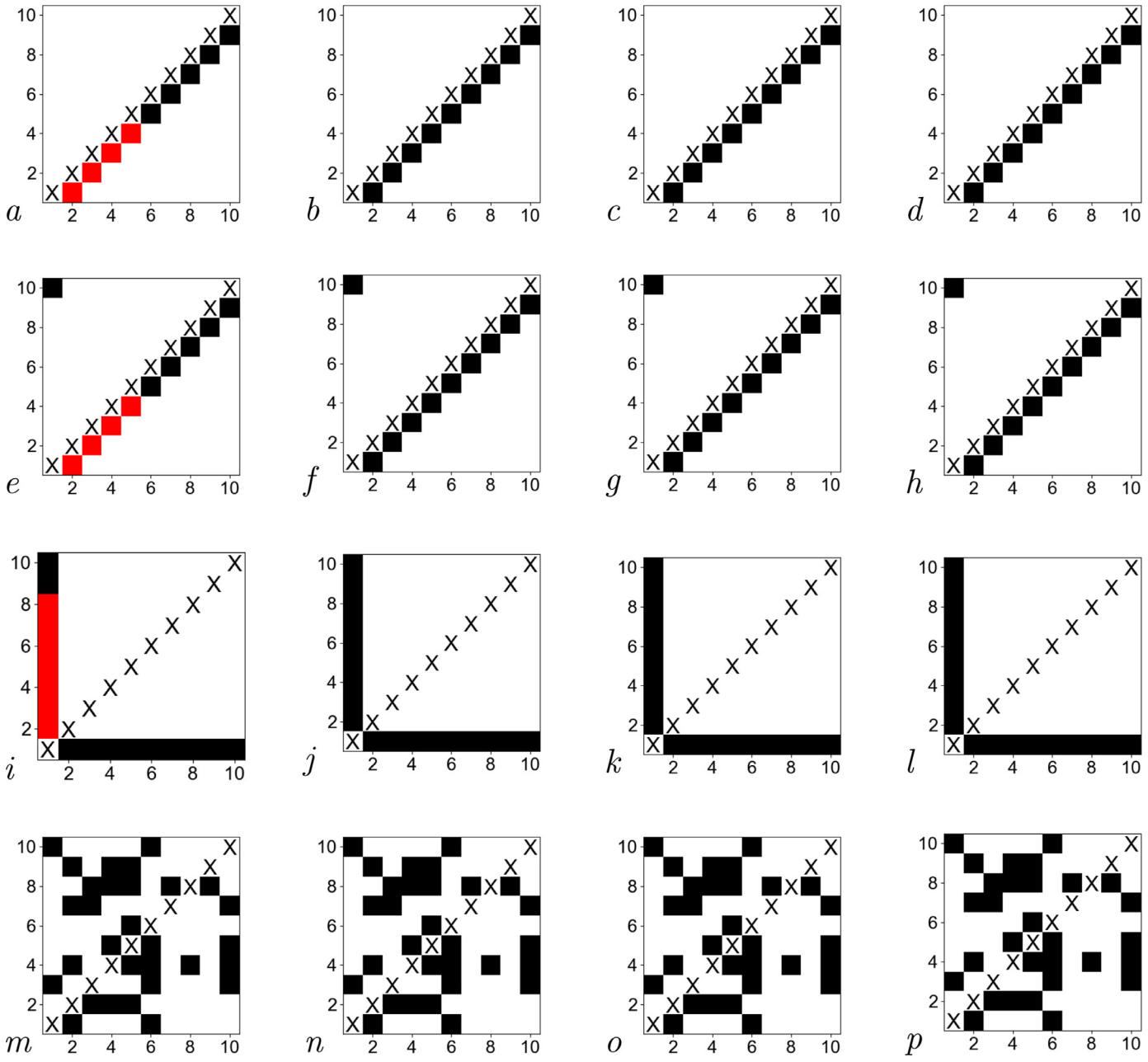

Fig. 4. Schemes of coupling architecture reconstruction using the method of elimination of couplings in the presence of 1% measurement noise. The first, second, third, and fourth lines correspond to the chain (*a*–*d*), ring (*e*–*h*), star (*i*–*l*), and random architecture (*m*–*p*), respectively. The first, second, third, and fourth rows correspond to the quasiharmonic (*a*), (*e*), (*i*), and (*m*), spiking (*b*), (*f*), (*j*), and (*n*), bursting (*c*), (*g*), (*k*), and (*o*), and chaotic (*d*), (*h*), (*l*), and (*p*) regimes, respectively. The numbers of driving neurooscillators are shown on the horizontal axis, while the numbers of driven oscillators are shown on the vertical axis. The squares of different color correspond to detected existing couplings (black), removed from the model nonexisting couplings (white), absent by definition couplings to itself at $j = i$ (cross) and missed existing couplings (red). (For interpretation of the references to colour in this figure legend, the reader is referred to the web version of this article.)

ate 1% noise the sensitivity is 44% for the quasiharmonic regime and 100% for the other regimes. The coupling to the central element in the star is not detected in most cases except one, see Fig. 3*i*. At the same time, the coupling from this element is always reconstructed successfully except quasiharmonic regime, in which the number of missed couplings increases with the increase of noise level. In the bursting and chaotic regimes, there are a lot of false positives in the opposite direction for ring and chain architectures, see. Fig. 3*c,d,g,h*. When the noise level is increased from 0% to 10%, the specificity remains approximately the same (68%–98%). The complexity of the coupling structure does not lead to better quality of the method.

The method of elimination of couplings in the absence of noise and at 1% noise level demonstrates 100% sensitivity and specificity for spiking, bursting, and chaotic regimes, see Fig. 4. The method specificity remains 100% at 5% and even at 10% noise levels as well. At 1%–5% noise levels, the method sensitivity is reduced (up to 55–61%) for the quasiharmonic regime, see Fig. 4(*a,e,i*). Moreover, with the increase of the coupling architecture complexity, the method becomes more sensitive. At the 10% noise level, the sensitivity drops for all regimes down to 0% for the bursting regime. As a result, as the coupling architecture becomes more complex, the method sensitivity increases, and the specificity of the method is always 100% for all the studied variants.

4. Conclusion and discussion

The proposed method is the result of further development of previously proposed approaches to reconstruction [19,20,34,38]. However, the method is applied to the network, which nodes are rather unique and have significant specifics, being at the same time the model of phased-locked loop system and neuron. This specifics of the network nodes can be useful for practical applications, especially in neuroscience and telecommunication.

The novelty of the work is as follows:

1. For the first time, a network of 3rd order systems with both unknown coupling architecture and unknown nonlinear function of each node was reconstructed using only scalar time series of individual nodes.
2. Since the individual node can provide a complex dynamics and qualitatively different regimes, including simple quasiharmonic oscillations, regular spikes and bursts, and chaotic behavior, the method was tested for all these regimes and showed its applicability.
3. The combination of numerical differentiation and integration was used for reconstruction of the state vector. The specifics of the proposed approach when a nonlinear function of one dynamical variable is not expanded in a row, but reconstructed as a table, allows to overcome the problem of unknown constant rising from numerical integration.
4. Two approaches to removal of superfluous coupling terms based on analytical properties of target function distribution were suggested and tested in all considered regimes.
5. For the first time, an impartial criterion to choose the number of points for smoothing the observable was proposed.
6. Specificity and sensitivity of the method were quantitatively estimated.
7. Different coupling architectures including chain, ring, star, and random architecture were considered, and specifics of reconstruction in each case was revealed. In particular, the appearance of false positives and false negatives occurred to be dependent on architecture. For example, the reconstruction of the architecture with one leading (central) node tends to omit most couplings in the direction to this nodes except most reliable. The chain and especially the ring architectures show maximal number of false positives in the pairs where there is an actual coupling in the opposite direction.

The proposed approach is highly resistant against the measurement noise and works well for coupling architecture reconstruction at noise levels up to 10%. The similar resistance to noise was previously reported for network reconstruction algorithms when additional special noise properties were assumed [39]. Such a significant resistance against noise was previously shown for reconstruction techniques dealing with first-order equations [20], but even for the second-order equation, the noise larger than 1% was often critical [19]. We assume that such robustness to noise is explained by the fact that the node nonlinear function is a function of phase. The function of phase is 2π-periodic by definition and cannot grow unlimited at the edges of the range as polynomials use to do. Besides, the phase is an antiderivative of the observable, therefore, it is resistant to noise as well as the target function, which depends on phase. Moreover, the new approach to choose the optimal smoothing parameter m can provide additional advantage.

In the star architecture, the special position of the central oscillator leads to asymmetry in the architecture reconstruction results: the coupling from this oscillator is usually reconstructed successfully, while the coupling to it is often missed. It is not surprising, since the impact of the central node into the dynamics of other nodes is very significant, while the impact of any other node into the dynamics of the central one is not large due to concurrency between them. Another possible reason can be the synchronization in the network and, therefore, similarity of oscillations of most nodes. Thus, when one peripheral node is incorporated into the model for the central node, it can imitate the other nodes by increasing the coupling coefficient. This hypothesis can be supported by the fact that sometimes one of peripheral nodes “replaces” the central element in the model for others, and it is always the node, the driving from which to the central node was detected.

In the present paper, we consider only one nonlinear function for each node and assume that the coupling functions are known, following the original works [22,23,33]. Since the method was developed for this model, we do not consider such limitations as shortcomings. However, in the case of the model extension, the explicit approximation of other functions can be used as in Refs. [19,20], providing possibility to use the proposed approach directly. Another possibility is to use the idea of iterative reconstruction of nonlinear functions described in Ref. [11].

In this study, the method of numerical differentiation and integration is used to obtain series of hidden variables following [1,5,6]. The other, even more popular approach is to use sequential time delays (lags) as it was proposed in Refs. [40] (in [41] more general case of nonuniform embedding was considered). It is very popular in a case when there is very few known about the evolution operator [2], including studies when partial directed coherence (PDC) [42] or conditional nonlinear Granger causality (GC) [43] is used to detect couplings in the ensemble. These techniques are more general than the proposed method and methods presented in Refs. [19,20,34,38] for specific systems, but the sensitivity and specificity of GC and PDC is much lower; e. g. the same systems were considered in Refs. [43,47] using GC and in Ref. [44–46] using PDC and in Refs. [19,38] using specific approaches. Therefore, use of specific approaches is mostly considered as preferable [2].

In the present study, the phase space reconstruction by means of delays approach is hardly to be applicable because the evolution operator is stated and the variables in the considered equations cannot be obtained one from another by means of time shift. There are other systems for which in some cases the proposed approach can be applicable with minimal changes, e. g. if we consider the Rössler system as it is rewritten in Ref. [6], and $\dot{x}$ is measured.

Declaration of Competing Interest

The authors declare that they have no known competing financial interests or personal relationships that could have appeared to influence the work reported in this paper.

CRediT authorship contribution statement

Marina V. Sysoeva: Investigation, Software, Validation, Visualization, Writing - original draft. **Ilya V. Sysoev:** Formal analysis, Conceptualization, Investigation, Writing - review & editing. **Mikhail D. Prokhorov:** Project administration, Writing - original draft, Writing - review & editing. **Vladimir I. Ponomarenko:** Methodology, Validation, Writing - original draft. **Boris P. Bezruchko:** Supervision, Resources, Funding acquisition.

Acknowledgment

This research was funded by the Russian Science Foundation, Grant No. 19-12-00201.

References

[1] Gouesbet G, Meunier-Guttin-Cluzel G, Menard O. Chaos and its reconstruction. New York: Nova Science Publishers; 2003. p. 320.

[2] Bezruchko BP, Smirnov DA. Extracting knowledge from time series. Berlin: Springer; 2010. p. 406.
[3] Aguirre LA, Letellier C. Modeling nonlinear dynamics and chaos: a review. Math Prob Eng 2009:238960.
[4] Wang WX, Lai YC, Grebogi C. Data based identification and prediction of nonlinear and complex dynamical systems. Phys Rep 2016;644:1–76.
[5] Gouesbet G, Letellier C. Global vector-field reconstruction by using a multivariate polynomial l2 approximation on nets. Phys Rev E 1994;49:4955–72.
[6] Besruchko BP, Smirnov DA. Constructing nonautonomous differential equations from experimental time series. Phys Rev E 2000;63:016207.
[7] Prokhorov MD, Ponomarenko VI. Estimation of coupling between time-delay systems from time series. Phys Rev E 2005;72:016210.
[8] Smirnov DA, Bezruchko BP. Detection of coupling in ensembles of stochastic oscillators. Phys Rev E 2009;79:046204.
[9] Navrotskaya EV, Smirnov DA, Bezruchko BP. The reconstruction of the couplings structure in the ensemble of oscillators according to the time series via phase dynamics modeling. Izvestiya VUZ Appl Nonlinear Dyn 2019;27(1):41–52.
[10] Zhang Y, Li H, Zhang Z, Qian Y, Pandey V. Network reconstruction from binary-state time series in presence of time delay and hidden nodes. Chin J Phys 2020;67:203–11.
[11] Cestnik R, Rosenblum M. Reconstructing networks of pulse-coupled oscillators from spike trains. Phys Rev E 2017;96(1):012209.
[12] Anishchenko VS, Pavlov AN, Janson NB. Global reconstruction in the presence of a priori information. Chaos Solitons Fractals 1998;9(8):1267–78.
[13] Casadiego J, Maoutsa D, Timme M. Inferring network connectivity from event timing patterns. Phys Rev Let 2018;121(5):054101.
[14] Shandilya SG, Timme M. Inferring network topology from complex dynamics. New J Phys 2011;13(1):013004.
[15] Casadiego J, Nitzan M, Hallerberg S, Timme M. Model-free inference of direct network interactions from nonlinear collective dynamics. Nat Commun 2017;8:2192.
[16] Han X, Shen Z, W-X W, Di Z. Robust reconstruction of complex networks from sparse data. Phys Rev Lett 2015;114:28701.
[17] Brunton SL, Proctor JL, Kutz JN. Discovering governing equations from data by sparse identification of nonlinear dynamical systems. Proc Nat Acad Sci USA 2016;113:3932–7.
[18] Mangan NM, Brunton SL, Proctor JL, Kutz JN. Inferring biological networks by sparse identification of nonlinear dynamics. IEEE Trans Mol Biol Multi-Scale Commun 2016;2:52–63.
[19] Sysoev IV. Reconstruction of ensembles of generalized Van der Pol oscillators from vector time series. Physica D 2018;384–385:1–11.
[20] Sysoev IV, Ponomarenko VI, Prokhorov MD. Reconstruction of ensembles of nonlinear neurooscillators with sigmoid coupling function. Nonlinear Dyn 2019;95(3):2103–16.
[21] Belyustina LN, Shalfeev VD. Theory of a nonlinear system of automatic phase-frequency control. Radiophys Quantum Electron 1968;11:213–20.
[22] Mishchenko MA, Shalfeev VD, Matrosov VV. Neuron-like dynamics in phase-locked loop. Izvestiya VUZ Appl Nonlinear Dyn 2012;20(4):122–30.
[23] Matrosov VV, Mishchenko MA, Shalfeev VD. Neuron-like dynamics of a phase-locked loop. Eur Phys J Spec Top 2013;222(10):2399–405.
[24] FitzHugh R. Mathematical models of threshold phenomena in the nerve membrane. Bull Math Biophysics 1955;17(4):257–69.
[25] Morris C, Lecar H. Voltage oscillations in the barnacle giant muscle fiber. Biophys J 1981;35(1):193–213.
[26] Hindmarsh JL, Rose RM. A model of the nerve impulse using two first-order differential equations. Nature 1982;296(5853):162–4.
[27] Dmitrichev AS, Kasatkin DV, Klinshov VV, Kirillov SY, Maslennikov OV, Shchapin DS, et al. Nonlinear dynamical models of neurons: review. Izvestiya VUZ Appl Nonlinear Dyn 2018;26(4):5–58.
[28] Lüttjohann A, H-C P. Regional specificity of cortico-thalamic coupling strength and directionality during waxing and waning of spike and wave discharges. Sci Rep 2019;9:2100.
[29] Pikovsky A. Reconstruction of a neural network from a time series of firing rates. Phys Rev E 2016;93:062313.
[30] Baake E, Baake M, Bock HG, Briggs KM. Fitting ordinary differential equations to chaotic data. Phys Rev A 1992;45(8):5524–9.
[31] Bezruchko BP, Smirnov DA, Sysoev IV. Identification of chaotic systems with hidden variables (modified Bock's algorithm). Chaos Solitons Fractals 2006;29:82–90.
[32] Sysoev IV, Ponomarenko VI, Bezruchko BP, Prokhorov MD. Reconstruction of parameters and unobserved variables of a semiconductor laser with optical feedback from intensity time series. Phys Rev E 2020;101(4):042218.
[33] Mishchenko MA, Bolshakov DI, Matrosov VV. Instrumental implementation of a neuronlike generator with spiking and bursting dynamics based on a phase-locked loop. Tech Phys Lett 2017;43:596–9.
[34] Sysoev IV, Prokhorov MD, Ponomarenko VI, Bezruchko BP. Reconstruction of ensembles of coupled time-delay system from time series. Phys Rev E 2014;89:062911.
[35] Molkov YI, Mukhin DN, Loskutov EM, Timushev RI, Feigin AM. Prognosis of qualitative system behavior by noisy, nonstationary, chaotic time series. Phys Rev E 2011;84:036215.
[36] Mukhin DN, Feigin AM, Loskutov EM, Molkov YI. Modified bayesian approach for the reconstruction of dynamical systems from time series. Phys Rev E 2006;73:036211.
[37] Hodgkin A, Huxley A. A quantitative description of membrane current and its application to conduction and excitation in nerve. J Physiol 1952;117:500–44.
[38] Sysoev IV, Ponomarenko VI, Kulminskiy DD, Prokhorov MD. Recovery of couplings and parameters of elements in networks of time-delay systems from time series. Phys Rev E 2016;94(5):052207.
[39] Zhang Z, Chen Y, Mi Y, Hu G. Reconstruction of dynamic networks with time-delayed interactions in the presence of fast-varying noises. Phys Rev E 2019;99(4):042311.
[40] Packard NH, Crutchfield JP, Farmer JD, Shaw RS. Geometry from a time series. Phys Rev Lett 1980;45(9):712–16.
[41] Kougioumtzis D. State space reconstruction parameters in the analysis of chaotic time series - the role of the time window length. Physica D 1996;95(1):13—28.
[42] Baccala LA, Sameshima K, Takahashi DY. Generalized partial directed coherence. In: Proceedings of the 2007 15th international conference on digital signal processing; 2007. p. 163–6.
[43] Chen Y, Rangarajan G, Feng J, Ding M. Analyzing multiple nonlinear time series with extended Granger causality. Phys Lett A 2004;324(1):26–35.
[44] Astakhova DI, Sysoeva MV, Sysoev IV. Effect of nonlinearity on coupling estimations between oscillators using partial directed coherence approach. Izvestiya VUZ Appl Nonlinear Dyn 2019;27(6):8–24.
[45] Sommerlade L, Eichler M, Jachan M, Henschel K, Timmer J, Schelter B. Estimating causal dependencies in networks of nonlinear stochastic dynamical systems. Phys Rev E 2009;80(5):051128.
[46] Schelter B, Timmer J, Eichler M. Assessing the strength of directed influences among neural signals using renormalized partial directed coherence. J Neurosci Methods 2009;179:121–30.
[47] Kornilov MV, Sysoev IV. Recovering the architecture of links in a chain of three unidirectionally coupled systems using the Granger-causality test. Tech Phys Lett 2018;44(5):445–9.